

Data-driven Policy Transfer with Imprecise Perception Simulation

Martin Pecka^{1,2}, Karel Zimmermann¹, Matěj Petrlík¹ and Tomáš Svoboda¹

Abstract—This paper presents a complete pipeline for learning continuous motion control policies for a mobile robot when only a non-differentiable physics simulator of robot-terrain interactions is available. The multi-modal state estimation of the robot is also complex and difficult to simulate, so we simultaneously learn a generative model which refines simulator outputs. We propose a *coarse-to-fine* learning paradigm, where the coarse motion planning is alternated with imitation learning and policy transfer to the real robot. The policy is jointly optimized with the generative model. We evaluate the method on a real-world platform in a batch of experiments.

I. INTRODUCTION

High-dimensional reactive motion control of complex unmanned ground robots which substantially interact with unstructured terrain is complicated. Main difficulties are threefold: (i) the sample inefficiency and local optimality of state-of-the-art reinforcement learning methods make direct policy optimization on a real platform inconceivable, (ii) the curse of dimensionality of planning methods [1] makes direct search prohibitively time-consuming, and (iii) the simulation inaccuracy of robot–terrain interactions often makes direct usage of simulator-learned policies impossible [2]. We propose a complete policy learning–planning–transfer loop, which addresses all of these issues simultaneously.

The aim of this work is to learn motion control policy for four independently articulated flippers of a tracked skid-steering robot shown in Figure 2. The proposed method exploits an analytically non-differentiable dynamics-engine-based simulator of the real platform [3]. The learned policy maps the local height map and pose of the robot to desired motion of the flippers, which assures smooth traversal over complex unstructured terrain.

The complexity of track–terrain interactions [3] slows the simulation speed down to real-time, therefore collecting a huge number of samples needed for accurate learning is impossible. Consequently, we propose coarse-to-fine policy learning, where the coarse motion planning is alternated with imitation learning and policy transfer to the real robot.

The proposed method starts by planning trajectories, which approximately optimize traversal of randomly generated terrains. Then imitation learning provides a coarse initial policy. Since it is impossible to simulate the state estimation described in Section IV accurately, the state estimated on the real platform significantly differs from the simulated state, and the real trajectories consequently suffer from substantial covariate shift. Instead of precise simulation, we

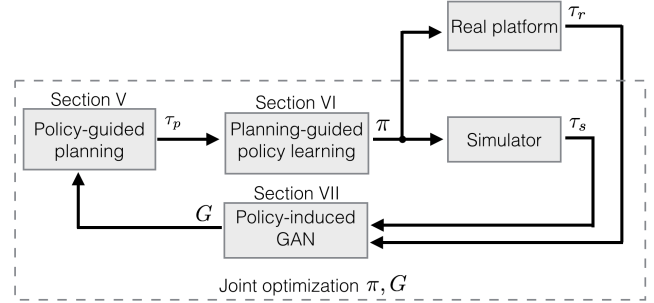


Fig. 1. **Proposed coarse-to-fine policy learning paradigm:** the coarse policy-guided motion planning is alternated with imitation learning and policy transfer to the real robot.



Fig. 2. **Robot surmounting unstructured terrain during USAR mission.**

suggest learning a conditional generative model of the state estimation procedure, which comprises both the underlying noise of different sensors and the errors caused by fusion of multi-modal measurements. This generative model is jointly optimized with the policy in order to simultaneously achieve both a trustworthy generative model and a well performing control policy on the real platform. In addition to that, the successively learned policy allows to guide the node expansion during planning which helps to obtain more accurate plans faster. This procedure is iterated until convergence.

Contribution of the paper lies in proposing the new self-contained learning–planning–transfer loop which simultaneously learns and transfers the policy using the generative model, which refines imprecise perception in simulation. The method is evaluated on a real platform.

II. RELATED WORK

We discuss three paradigms relevant to our approach: (i) transfer of policies learned on a black-box simulator, (ii) learning policies on a differentiable motion model estimated solely from real trajectories, and (iii) data-driven refinement of perception simulator.

¹Czech Technical University in Prague, Faculty of Electrical Engineering, Department of Cybernetics

²Czech Technical University in Prague, Czech Institute of Informatics Robotics and Cybernetics

Direct policy transfer methods: Oswald et al.[4] demonstrated direct transfer of motion navigation policy for Nao humanoid robot. Policy was first learned in simulation, where everything was carefully modeled as close to reality as possible. The simulation involved motion blur and feature detection noise. Finally, the policy was directly used on the real platform and performed well thanks to precise simulation. In our case, precise simulation of the perception and motion of the ground robot on an uneven terrain is not easy to achieve. Nevertheless, using the simulator for initialization seems useful. Nemeč et al. [5] used value function learned in simulation to bootstrap the real robot learning. We also initialize the policy from the simulator.

Model-based reinforcement learning methods learn simultaneously model and the policy. Since the model learned from the scratch on real trajectories is typically a fast differentiable function [6], [7], direct policy optimization is often possible. We argue that learning the policy for robot–terrain interaction with high-dimensional state space such as height map is impossible this way. Main difficulties arise from the fact that learning the motion and perception model from real trajectories (i) endangers the robot and (ii) requires prohibitively high number of trajectories for reliable learning. In contrast to these approaches, we already make use of a sophisticated motion model, and mainly focus on the perception transfer.

Data-driven refinement of perception simulator: The problem of transferring perception between different domains is well studied. In computer vision Generative Adversarial Nets [8] (GANs) have been recently used for generating synthetic training images. Shrivastava et al. [9] have shown significant performance boost if GANs are used to refine graphics-engine–based images. Similarly, we also refine simulator-generated data. In contrast to these works, we do not simulate a single sensor but the result of a complete SLAM pipeline which is difficult to model.

III. PIPELINE OVERVIEW

Our pipeline follows three main assumptions typical for robot–terrain simulations: (i) both the physics-based simulator is slow and analytically non-differentiable, (ii) simulation of the exteroceptive perception such as mapping from multi-modal sensor fusion is not realistic, and (iii) there exists an unknown generative model G which corrects the simulated perception to be close to the real perception. Under these assumptions, we search for control policy π^* , which minimizes the expected sum of traversal costs c of the real robot.

Let us denote p_r^π the probability distribution of trajectories $\tau_r = \{(\mathbf{x}_r^i, \mathbf{a}_r^i)\}_i$ generated by the real robot under policy π , and $p_s^\pi(G)$ the probability distribution of trajectories τ_s generated by the simulator with generative model G under policy π . We search for policy

$$\pi^* = \arg \min_{\pi} \mathbb{E}_{\tau_r \sim p_r^\pi} \{c(\tau_r)\} \quad (1)$$

Using assumption (iii), we rewrite the optimization problem using the simulator distribution $p_s^\pi(G)$ in the objective

as follows

$$\arg \min_{\pi, G} \{\mathbb{E}_{\tau_s \sim p_s^\pi(G)} \{c(\tau_s)\} \mid \text{s.t. } p_s^\pi(G) = p_r^\pi\}. \quad (2)$$

Since trajectories collected with the simulator and with the real robot are unpaired, direct supervised training of the generative model is impossible. Consequently, we replace constraint $p_s^\pi(G) = p_r^\pi$ by the saddle point constraint on GAN-like loss $\mathcal{L}_{\text{GAN}}(G, D, \pi)$ induced under policy π

$$\begin{aligned} \arg \min_{\pi, G} \mathbb{E}_{\tau_s \sim p_s^\pi(G)} \{c(\tau_s)\} \\ \text{s.t. } G = \arg \min_{G'} \max_D \mathcal{L}_{\text{GAN}}(G', D, \pi), \end{aligned} \quad (3)$$

where D denotes a discriminator.

If the GAN loss $\mathcal{L}_{\text{GAN}}(G, D, \tau_r, \tau_s)$ is pure GAN loss [8]

$$\mathbb{E}_{\tau_r \sim p_r^\pi} \log D(\tau_r) + \mathbb{E}_{\tau_s \sim p_s^\pi(G)} \log(1 - D(G(\tau_s))),$$

the saddle-point generator provides samples from the true distribution and the equivalence between eq. (2) and eq. (3) holds. In order to achieve fast convergence on the high-dimensional unpaired data, we use CycleGAN loss [10], therefore eq. (3) is an approximation of the original problem.

By assumption (i), any direct optimization of eq (3) is technically intractable. We propose approximated optimization scheme, which minimizes the interaction with the slow simulator and the real robot.

The optimization alternates between (i) planning guiding samples τ_p , which approximately optimize objective

$$\arg \min_{\tau_p} \mathbb{E}_{\tau_p'} \{c(\tau_s)\}, \quad (4)$$

(ii) collecting real and simulated trajectories τ_r, τ_s , and (iii) searching for the control policy and the generative model which minimize the locally approximated criterion

$$J(\pi, G, \tau_p) = \sum_{(\mathbf{x}, \mathbf{a}) \in \tau_p} \|\pi(G(\mathbf{x})) - \mathbf{a}\| \quad (5)$$

subject to locally approximated GAN loss $\mathcal{L}_{\text{GAN}}(G, D, \tau_r, \tau_s)$ around the collected trajectories τ_r, τ_s . The proposed pipeline is summarized in Figure 1 and Algorithm 1.

The generative model G^0 is initialized as identity. The initial policy π^0 is initialized by imitation learning (i.e. we plan initial trajectories τ_p and estimate $\pi^0 = \arg \min_{\pi} J(\pi, G^0, \tau_p)$). Given the initial policy, real trajectories are collected and alternated optimization (lines 3–8) with K iterations is performed. Finally, a new set of real test trajectories is collected and the whole process is repeated until a satisfactory behavior of the real robot is observed.

IV. REAL PLATFORM AND ITS SIMULATION MODEL

The real robot used in our experiments is the Absolem tracked vehicle used in Urban Search and Rescue scenarios [11], which is depicted in Figure 3. It is equipped with a gyro providing its spatial orientation and with a rotating 2D lidar which provides full 3D laser scans at rate 0.3 Hz. The point map built from lidar scans by the state-of-the-art

Algorithm 1 Overview of the real policy learning

- 1: **Initialize:** G^0 as identity and policy π^0 .
 - 2: **Collect** real trajectories $\tau_r \sim p_r^{\pi^0}$
 - 3: **for** $k = 0 \dots K$ **do**
 - 4: **Plan** guiding traj. τ_p^k biased by π^k (Section V).
 - 5: **Optimize** policy w.r.t. new generator (Section VI)
 $\pi^{k+1} = \arg \min_{\pi} J(\pi, G^k, \tau_p)$
 - 6: **Collect** simulated trajectories: $\tau_s^{k+1} \sim p_s^{\pi^{k+1}}(G^k)$
 - 7: **Find** trajectory-consistent saddle point (Section VII)
 $G^{k+1} = \arg \min_G \max_D \mathcal{L}_{GAN}(G, D, \tau_r, \tau_s^{k+1})$
 - 8: **end for**
 - 9: $G^0 = G^K$, $\pi^0 = \pi^K$ and **repeat** from line 2.
-

SegMatch algorithm [12] is combined with high-precision track odometry in a multi-modal fusion pipeline [13].

For simulation, we use our custom tracked vehicle dynamics model implemented in the Gazebo simulator [3]. We showed that although it is a good approximation of motion of the tracked vehicle, it is not a perfect simulation of the real world. Parts of the simulation are randomized or pseudo-randomized (e.g. search of contact points of colliding bodies, solving of the underlying dynamics equations), so every execution of even a deterministic policy results in slightly different outcomes. This is useful for us, because otherwise artificial noise would have to be added to generate a multitude of different trajectories using one control policy. To achieve fast simulation, several simplifications were implemented in the simulated perception pipeline, and the policy inputs were selected to be easy to obtain both in reality and in the simplified simulator.

The most important of all policy inputs is the *Digital Elevation Map* (DEM) of close robot neighborhood (visualized in Figure 3). It is a horizontal 2D grid of rectangular cells where each cell contains information about the highest 3D point located in it. When there is no point measured inside a cell, a *Not-a-number* (NaN) value is stored. The DEM is treated in the coordinate frame of the robot with pitch and roll angles zeroed out. On the real robot, DEM is constructed from the point map. In simulation, DEM measurement is done in a completely different way to avoid inefficient laser ray-tracing: we directly extract the height of the highest object (excluding robot body) in each DEM cell, which is a fast operation. That means there are no missing measurements in the simulator DEM, and also no noise.

The simplification in the perception pipeline allows us running the simulator achieving real-time speeds. That allows generating hundreds of trajectories in the simulation. Execution of the policies on the real robot is even more time-consuming, which means only tens of trajectories are realistic to be performed.

V. GENERATING GUIDING PLANS

The simulator is utilized by the path planner to sample trajectories τ_p^k , which are further used in the pipeline as

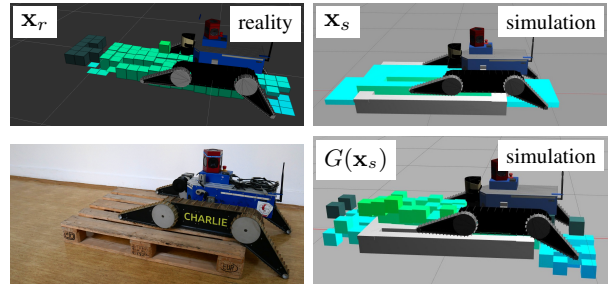


Fig. 3. **Real and simulated DEMs.** A visualization of Digital Elevation Maps (DEMs) is shown above. Dark green cells represent NaNs. Both vertical position and color of the cells visualize the height of the respective DEM cell. **Top left:** DEM captured by the real platform. **Bottom left:** The real pose of the robot on an obstacle. **Top right:** DEM from simulator. The shapes are ideal and all measurements are available. **Bottom right:** DEM from simulator transformed by G to appear realistic.

described in Algorithm 1.

The planner works on a multitude of randomly generated worlds (*training worlds*) with different obstacles, corresponding approximately to the expected real obstacles. Each training world has a predefined length of trajectories the robot has to *safely* traverse to consider the trajectories *close-to-optimal* (a time limit is also in place to cut off plans stuck in local optima).

Different definitions of *close-to-optimal* trajectories can be used; they are always closely related to the particular task. In our case, multiple actions can be desired in some situations, which prevents definition of an explicit reward function. Instead, we utilize the fact that if the flippers are controlled incorrectly, the robot is not able to overcome obstacles and gets stuck or damaged. Safety of trajectories is given by several criteria like maximum allowed accelerations, limits on pitch and roll angles, and parts of the robot body which cannot touch any part of the environment (like the fragile sensors). It is also possible to impose other constraints on the trajectories this way.

Input of the planner consists of the training world specification and guiding policy π . The task is to find a close-to-optimal trajectory τ satisfying the constraints described above while keeping planned actions as close to actions of π as possible (except for the initial iteration without guiding).

The planner uses an RRT-based algorithm of state space search. Each action (target flipper configuration) expansion in a planning node is evaluated in the simulator and a new planning node is created for the returned state. Even though a standard RRT planner can find a solution by exploring the state space uniformly in all dimensions, in reality it is often impractical as the search requires a number of iterations which grows with the volume of the search space. In high-dimensional applications, especially when each expansion is costly due to real-time simulation times as in our case, a heuristic must be employed to reduce the required iterations. One general approach is guiding the growth of the tree towards the goal state, without getting stuck in an obstacle which is typically realized by a geometric path obtained in a simplified search space [14], [1]. This path is then refined

by the guided RRT planner with expansions respecting all kinematic and dynamic constraints of the motion model. We propose to start the planning in a reduced action space (a small number of allowed actions, lower time resolution) which is practical to be explored (but yields trajectories which would not be desired/close-to-optimal optimal in the full action space).

An essential speedup of the planner is available once the first iteration of the proposed pipeline is finished and a control policy has been found. This policy is used as the heuristics. Since policy π_{i-1} represents the previous set of trajectories τ_p^{i-1} with some model error, the path planner guided by it in iteration i will generate actions that are different from the actions in iteration $i-1$. An important property of this heuristics is that with more planning-learning iterations, the plans will be closer to the subspace representable by the chosen policy class, which should in return result in better fit of future policies to future planned paths. The speedup gained by the guiding is for the possibility to enlarge the searched action space or refine the time resolution.

VI. IMITATION LEARNING

With a set of trajectories generated by the path planner, the imitation learning phase can start. Generally, it is possible to use any kind of supervised learning in this part. We chose a deep neural network that is crafted to make use both of the 2D structure of DEMs and to handle correctly *Not-a-Number* (NaN) values.

Inputs to the network are DEM, orientation of the robot and current flipper positions. It outputs 4 desired flipper positions. Normally, if a NaN value would enter as a part of the DEM, it would silently spread further and could eventually end up in one of the outputs, which is undesirable.

A standard approach is to replace NaNs with a neutral value (like 0). We argue that it might change the characteristics of the measurements. We decided to treat the NaN values as “first-class citizen” in the network because they can also carry useful information (the fact that a measurement is missing).

We propose the following input processing: the DEM is converted into two matrices of the same shape—one with NaNs replaced by zeros, and the other with ones in measured cells and zeros in cells with NaNs (this part of architecture is shared with the GANs described in Section VII). Each of these matrices is fed into its own convolutional layer, and their outputs are multiplied. This effectively means normalizing each patch covered by a convolutional filter by the number of measured values in this patch. From this layer on, no NaN values are in the network, the output of the convolution is flattened, concatenated with the 1D inputs (robot orientation, flipper angles) and finally enters a fully connected layer, whose output are the four desired flipper angles.

The regressor network is trained using a standard algorithm (Adam optimizer with gradient clipping) to minimize the error between the predicted flipper target positions and

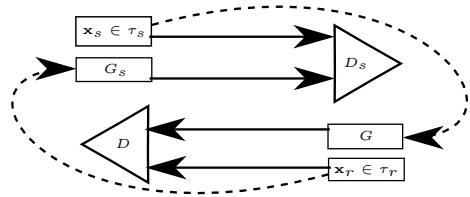


Fig. 4. **CycleGAN architecture.** Two GAN networks interconnected in such a way that input dimension of generator G_s is the same as output dimension of G and vice versa. The discriminators D_s and D serve both for evaluation of single generator loss and the cyclic loss.

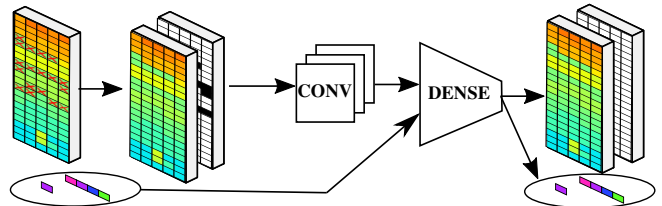


Fig. 5. **Generator architecture.** Generators G_s and G share the same architecture in our experiments, although it is not a general requirement. The raw input consists of a 20×5 DEM representation possibly containing NaN values, and 5 angles – robot pitch and the 4 flipper angles. The raw input is preprocessed to yield a tensor of shape $21 \times 5 \times 2$ which is then used by the rest of the network.

those provided in the dataset. The dataset is randomly divided into training and test parts and quality assessment of the planning is based on the test error.

VII. DATA TRANSFORMATION VIA CGANS

The next key step is to find a suitable transformation between the data observed on the real platform and data observed in the simulator.

CycleGANs [10] were shown to be useful in the task of mutual mapping of two domains when only unpaired data are available. Specifically, Shrivastava et al. [9] used them to transform a simulated dataset to look real and then applied standard deep learning that expects real data at the inputs. An advantage of this approach is that it yields both transformations from simulated data to real and vice versa.

The mapping from simulated to real data realized by generator G is better conditioned because it takes full DEMs, applies noise, and masks out cells that should not be observable. The other process represented by generator G_s has inherent problems with choosing the right values to fill in the places where measurements are missing (since many values may come in the place of one NaN). The relation between the generators, their discriminators and input datasets is shown in Figure 4

The input data with special structure (20×5 2D data possibly containing NaNs + 5 scalar constants), are preprocessed similar to Section VI. In generators and discriminators, the input DEM is transformed into a $20 \times 5 \times 2$ tensor where the first channel contains the DEM with NaNs substituted with 0s and the second channel contains a mask with -1 s at NaN cells in the DEM, and 1s otherwise.

The scalar inputs (robot orientation and flipper angles) skip these first convolution layers and enter the network later as inputs to a fully connected layer. At the output, the DEM and the scalar values are again separated. This allows the network to work as a standard image-to-image CycleGAN, but also allows it to use the scalar information.

The internal structure of the generators and discriminators contains several convolution layers that retain dimension of their inputs and use the Leaky ReLU activation function, and a final fully-connected layer.

Our pipeline suggests that the generators should be initialized to identity, which is not generally possible with neural networks containing non-linear activation functions. However, implementing a skip-connection of the input data directly to the fully-connected layer allows this initialization. Identity should be a good initial guess for the generator, because we do not want it to change the data too much.

Both discriminators use the pure GAN loss formulation (see Section III).

Loss function of both generators is defined in means of their corresponding discriminator (D for generator G ; D_s for generator G_s):

$$\mathcal{L}_G(\mathbf{x}) = +\lambda \cdot \sum (\log(D(\mathbf{x}))) + \lambda_p \cdot \sum_i \|\mathbf{x}_i - G(\mathbf{x}_i)\|$$

We penalize distance of the generated output from the inputs (pixel-wise), as it was shown to stabilize the learning [9] and we indeed want the generator to do minimum modifications to its input, as long as it is able to fool the discriminator. One additional component of \mathcal{L}_{G_s} can be added that penalizes any NaN values in the output, since we know there are no NaNs in the simulator DEMs.

The cycle loss $\mathcal{L}_c(G, D, \mathbf{x}_r, G_s, D_s, \mathbf{x}_s)$ is defined as

$$\mathcal{L}_D(G(G_s(\mathbf{x}_r))) + \mathcal{L}_{D_s}(G_s(G(\mathbf{x}_s)))$$

Training of the network is done by repeated optimization of all generator and discriminator losses, where $\lambda_c \cdot \mathcal{L}_{cycle}$ is added to the loss of both generators. The training is done on simulated data from τ_s^k and real data from τ_r .

VIII. EXPERIMENTS

Experimental evaluation of the learned policies is an essential part of the learning loop. After several iterations of the learning, planning and generator optimization, verification in the real world is to be performed.

For the task of terrain traversal with a tracked robot, we designed a real test scenario consisting of flat ground, a pallet and a staircase, which are typical obstacles the robot can encounter during search&rescue missions. The staircase is subdivided to 6 sections with different characteristics – approach to stairs, on stairs, leaving stairs, and the stairs can go either upwards or downwards. The staircase is traversed with constant forward speed 0.3 m/s three times and the pallet 10 times, resulting in execution of 13 trajectories with duration about 5 real-world minutes. Every trajectory is assigned one of three success levels – *good* in case the trajectory was without problems, the robot passed and did not

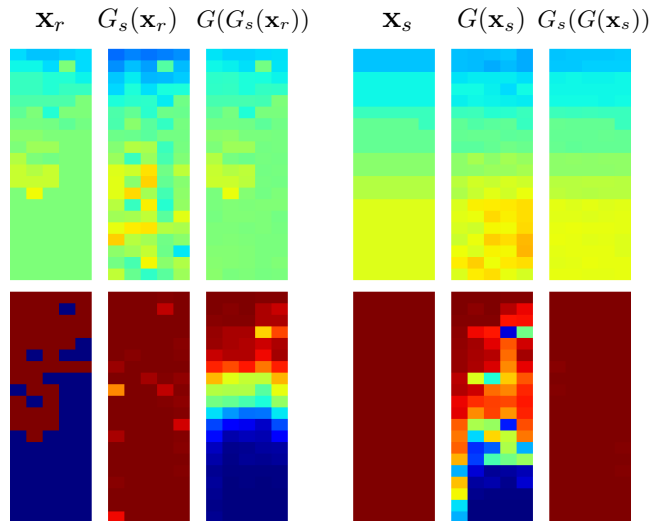


Fig. 6. DEMs transformed by the generators. **Top:** heights in the DEM (blue = -1, green = 0, red = +1). **Bottom:** corresponding NaN masks (blue = NaN, red = not NaN).

endanger itself; *unclear* if there were minor problems during the execution, but the robot traversed the whole required length (e.g. behavior close to unsafe, the operator had to reduce the otherwise constant travel speed, and so on); finally *fail* level is assigned to trajectories that the robot could not finish or executed an unsafe action (a safety person is following the robot and prevents the worst consequences of such actions). These levels carry numerical value (*good* = 1.0, *unclear* = 0.5, *fail* = 0.0) and policy performance is an average of these values over all executions.

Similar obstacles were modeled in the simulator and a set of 8 test worlds was created. The metrics for simulation is proportion of *good* trajectories among all executed. Here *good* means traversing the required length of the trajectory with constant speed 0.3 m/s without executing any unsafe actions (as described in Section IV).

Results of the learning process are summarized in Table I and Table II. Testing in real world started in the fourth simulated iteration, when the policy became efficient in simulation. In each imitation learning instance, we trained 10 policies and chose two that evaluated best on the simulated test worlds. These two policies were tested in real world as described above and the better one became π^{k+1} .

We cut off the whole pipeline once the policy achieved good performance in the real world (after 7 iterations). That accounts for ca 15 minutes of driving with the real robot to collect the initial τ_r , then 4×13 trajectories for real-world policy verification, which is about 20 minutes. No more real-world execution was needed.

Summing up the computation time, we needed 800 CPU-core-hours (of which 90% is spent on performance verification, which could be lowered) and 50 GPU-hours (highly depends on structures of the policy and GANs).

A video of testing the trained policies on really unstructured terrain is available on our website <http://cmp>.

TABLE I
AVERAGE POLICY PERFORMANCE IN SIMULATION

Simulation test worlds									
Iter	1	2	3	4	5	6	7	8	Σ
Only simulation									
1	0.05	0.00	0.00	0.81	0.16	0.15	1.00	1.00	3.17
2	1.00	1.00	0.30	1.00	0.13	0.14	1.00	1.00	5.57
3	1.00	0.93	0.49	0.31	0.93	0.90	1.00	1.00	6.56
Simulation + real world									
4	0.03	0.44	0.52	0.87	0.80	0.50	1.00	1.00	5.16
5	0.60	0.79	0.43	0.16	0.99	0.98	1.00	1.00	5.95
6	1.00	0.50	0.66	1.00	0.52	0.52	1.00	1.00	6.20
7	1.00	1.00	0.57	1.00	0.69	0.56	1.00	1.00	6.82

TABLE II
AVERAGE POLICY PERFORMANCE IN REAL WORLD

Test obstacles in real world									
Iter	F	P	SU1	SU2	SU3	SD1	SD2	SD3	Σ
4	1.00	0.20	0.67	0.00	0.33	0.50	0.00	0.67	3.37
5	1.00	0.65	1.00	0.00	0.67	0.67	0.33	0.67	4.99
6	1.00	0.65	1.00	0.17	1.00	0.33	0.33	0.83	5.31
7	1.00	0.60	0.83	0.50	0.83	0.50	0.67	1.00	5.93

F = flat terrain, P = pallet, SU1 = approach stairs up, SU2 = on stairs up, SU3 = leave stairs up, SD1 = approach stairs down, SD2 = on stairs down, SD3 = leave stairs down. Maximum performance = 8.0.

felk.cvut.cz/~peckama2/policy_transfer/.

We also experimentally verified that guiding decreases path-planning time or allows to plan paths in more-dimensional spaces. A summary of computation times is shown in Table III. Notice the required time decreases with further iterations when parameters do not change, which shows that the policy is a good heuristic. The increase in planning time in the last iteration is because we collected new τ_r samples and retrained the generator on them, but the policy from iteration 6 was trained on a generator based on a different real dataset, which decreased performance of the policy as a heuristics. We also tried unguided planning with 200 ms resolution, but no path was found in one hour.

IX. CONCLUSION AND FUTURE WORK

We have proposed and experimentally evaluated the new self-contained learning–planning–transfer loop, which employs a simulator of robot–terrain interactions. The proposed method simultaneously learned the policy in simulation and transferred it to the real robot. The transfer was achieved by a generative model which corrected imprecisely simulated perception. The experimental evaluation showed that iterations of the learning–planning–transfer loop improve performance of the policy on the real robot. We also showed that it is possible to further refine the action space of guiding policies without compromising computational tractability.

Our ongoing research will focus on possibilities of making the CycleGAN learning policy-aware, so that the generators are trained with policy performance in mind.

TABLE III
PATH-PLANNING PERFORMANCE

Iter	Guided	Actions	Δt	Avg. CPU time
1	×	3	1000 ms	8 min
2	✓	3	1000 ms	5 min
3	✓	3	1000 ms	5 min
4	✓	7	1000 ms	15 min
5	✓	7	1000 ms	12 min
6	✓	7	200 ms	30 min
7	✓	7	200 ms	45 min
-	×	3	200 ms	$\gg 60$ min

CPU-core–time needed to sample one trajectory by the path planner. Δt is time resolution (i.e. with $\Delta t = 200$ a trajectory of some defined metric length needs $5\times$ more nodes than with $\Delta t = 1000$).

ACKNOWLEDGMENT

The research leading to these results has received funding from the European Union under grant agreement FP7-ICT-609763 TRADR; from the Czech Science Foundation under Project GA14-13876S, and by the Grant Agency of the CTU Prague under Project SGS16/161/OHK3/2T/13.

REFERENCES

- [1] D. Ferguson and A. Stentz, “Anytime RRTs,” in *IEEE/RSJ International Conference on Intelligent Robots and Systems*, October 2006, pp. 5369–5375.
- [2] J. Kober, “Learning motor skills: from algorithms to robot experiments,” in *Information Technology*, 2014.
- [3] M. Pecka, K. Zimmermann, and T. Svoboda, “Fast simulation of vehicles with non-deformable tracks,” in *2017 IEEE/RSJ International Conference on Intelligent Robots and Systems (IROS)*. IEEE, sep 2017, pp. 6414–6419.
- [4] S. Oswald, A. Hornung, and M. Bennewitz, “Learning reliable and efficient navigation with a humanoid,” in *International Conference on Robotics and Automation*, 2010.
- [5] B. Nemeč, M. Zorko, and L. Zlajpah, “Learning of a ball-in-a-cup playing robot,” in *International Workshop on Robotics*, 2010.
- [6] M. P. Deisenroth, D. Fox, and C. E. Rasmussen, “Gaussian Processes for Data-Efficient Learning in Robotics and Control,” in *IEEE Transactions on Pattern Analysis and Machine Intelligence*, 2014.
- [7] R. Tedrake, “LQR-trees: Feedback motion planning on sparse randomized trees,” in *Proceedings of Robotics: Science and Systems*, 2010.
- [8] I. Goodfellow, J. Pouget-Abadie, M. Mirza, B. Xu, D. Warde-Farley, S. Ozair, A. Courville, and Y. Bengio, “Generative adversarial nets,” in *Advances in Neural Information Processing Systems*, 2014, pp. 2672–2680.
- [9] A. Shrivastava, T. Pfister, O. Tuzel, J. Susskind, W. Wang, and R. Webb, “Learning from Simulated and Unsupervised Images through Adversarial Training,” in *Computer Vision and Pattern Recognition*, 2017.
- [10] J.-Y. Zhu, T. Park, P. Isola, and A. A. Efros, “Unpaired Image-to-Image Translation using Cycle-Consistent Adversarial Networks,” in *Computer Vision and Pattern Recognition*, 2017.
- [11] I. Kruijff et al., “Designing, developing, and deploying systems to support human-robot teams in disaster response,” *Advanced Robotics*, vol. 28, no. 23, pp. 1547–1570, 2014.
- [12] R. Dube, D. Dugas, E. Stumm, J. Nieto, R. Siegwart, and C. Cadena, “SegMatch: Segment based place recognition in 3D point clouds,” in *2017 IEEE International Conference on Robotics and Automation (ICRA)*, 2017, pp. 5266–5272.
- [13] J. Simanek, M. Reinstein, and V. Kubelka, “Evaluation of the EKF-based estimation architectures for data fusion in mobile robots,” *IEEE/ASME Transactions on Mechatronics*, vol. 20, no. 2, pp. 985–990, 2015.
- [14] V. Vonásek, J. Faigl, T. Krajník, and L. Přeučil, “A sampling schema for rapidly exploring random trees using a guiding path,” in *European Conference on Mobile Robots (ECMR)*, 2011, pp. 201–206.